Arteriosclerosis, Thrombosis, and Vascular Biology
JOURNAL OF THE AMERICAN HEART ASSOCIATION

Lysophosphatidic Acid Signaling Protects Pulmonary Vasculature From Hypoxia-Induced Remodeling

Hsin-Yuan Cheng, Anping Dong, Manikandan Panchatcharam, Paul Mueller, Fanmuyi Yang, Zhenyu Li, Gordon Mills, Jerold Chun, Andrew J. Morris and Susan S. Smyth

Arterioscler Thromb Vasc Biol 2012, 32:24-32: originally published online October 20, 2011
doi: 10.1161/ATVBAHA.111.234708
Arteriosclerosis, Thrombosis, and Vascular Biology is published by the American Heart Association. 7272 Greenville Avenue, Dallas, TX 72514
 Print ISSN: 1079-5642. Online ISSN: 1524-4636

Lysophosphatidic Acid Signaling Protects Pulmonary Vasculature From Hypoxia-Induced Remodeling

Hsin-Yuan Cheng, Anping Dong, Manikandan Panchatcharam, Paul Mueller, Fanmuyi Yang, Zhenyu Li, Gordon Mills, Jerold Chun, Andrew J. Morris, Susan S. Smyth

Objective—Lysophosphatidic acid (LPA) is a bioactive lipid molecule produced by the plasma lysophospholipase D enzyme autotaxin that is present at ≥100 nmol/L in plasma. Local administration of LPA promotes systemic arterial remodeling in rodents. To determine whether LPA contributes to remodeling of the pulmonary vasculature, we examined responses in mice with alterations in LPA signaling and metabolism.

Methods and Results—*Enpp2*$^{+/-}$ mice, which are heterozygous for the autotaxin-encoding gene and which have reduced expression of autotaxin/lysophospholipase D and approximately half normal plasma LPA, were hyperresponsive to hypoxia-induced vasoconstriction and remodeling, as evidenced by the development of higher right ventricular (RV) systolic pressure, greater decline in peak flow velocity across the pulmonary valve, and a higher percentage of muscularized arterioles. Mice lacking LPA_1 and LPA_2, 2 LPA receptors abundantly expressed in the vasculature, also had enhanced hypoxia-induced pulmonary remodeling. With age, *Lpar1*$^{-/-}$2$^{-/-}$ mice spontaneously developed elevated RV systolic pressure and RV hypertrophy that was not observed in *Lpar1*$^{-/-}$ mice or *Lpar2*$^{-/-}$ mice. Expression of endothelin-1, a potent vasoconstrictor, was elevated in lungs of *Lpar1*$^{-/-}$2$^{-/-}$ mice, and expression of $endothelin_B$ receptor, which promotes vasodilation and clears endothelin, was reduced in *Enpp2*$^{+/-}$ and *Lpar1*$^{-/-}$2$^{-/-}$ mice.

Conclusion—Our findings indicate that LPA may negatively regulate pulmonary vascular pressure through LPA_1 and LPA_2 receptors and that in the absence of LPA signaling, upregulation in the endothelin system favors remodeling. (***Arterioscler Thromb Vasc Biol.* 2012;32:24-32.**)

Key Words: lipids ■ pulmonary artery ■ pulmonary hypertension ■ autotaxin ■ lysophospahtidic acid

Arterial smooth muscle cells (SMCs) regulate vessel contraction and relaxation and, following systemic vascular injury, can undergo phenotypic modulation to a proliferative/synthetic state that likely contributes to the development of atherosclerosis and restenosis.[1] In the highly compliant pulmonary circulation, large changes in blood flow are accommodated with little alteration of pressure by tightly coordinated vasoactive mediators. Dysregulation in the balance between pulmonary vasodilators and vasoconstrictors can trigger pulmonary vascular remodeling, characterized by an increase in pulmonary SMC proliferation, hypertrophy, and the number of SMC-wrapped small arterioles. As a consequence, pulmonary hypertension (PH) with elevated pulmonary vascular resistance and sustained high pulmonary arterial pressure develops.[2–4] Endothelial dysfunction, including an increase in endothelial permeability and apoptosis, is associated with and likely promotes PH.[2,4,5] With time, the increase in pulmonary vascular resistance and pressure results in right ventricular (RV) hypertrophy, dilatation, and dysfunction.[4,6] Cardiopulmonary disorders associated with elevated pulmonary artery pressures are one of the leading causes of RV hypertrophy and failure.[7] Unfortunately, at present, very little is known about the mediators that initiate pulmonary vascular changes underlying PH, making prevention and effective treatment of the disease challenging.[8]

Lysophosphatidic acid (LPA) is a bioactive lipid molecule present in plasma concentrations (≥100 nmol/L) predicted to activate its signaling receptors.[9,10] LPA has effects on cultured SMCs and endothelial cells that make it an attractive candidate regulator of the pulmonary vasculature in vivo.[11] LPA is a potent autocrine regulator of phenotypic modulation of cultured vascular SMCs. Indeed, LPA has been proposed to be the major mediator in serum responsible for dedifferentiation of cultured vascular SMCs. Moreover, local administration of LPA in carotid arteries of rodents triggers a remodeling response, which requires SMC dedifferentiation and proliferation.[12–17] LPA may also have important effects on endothelial cell function and endothelial barrier stability.[18–20] In isolated cell systems, LPA has been reported to affect endothelial nitric oxide synthase activity and, conse-

Received on: July 12, 2011; final version accepted on: September 23, 2011.

From the Division of Cardiovascular Medicine, Gill Heart Institute, University of Kentucky, Lexington, KY (H.-Y.C., A.D., M.P., P.M., F.Y., Z.L., A.J.M., S.S.S.); Department of Systems Biology, University of Texas M.D. Anderson Cancer Center, Houston, TX (G.M.); Department of Molecular Biology, Scripps Research Institute, San Diego, CA (J.C.); Department of Veterans Affairs Medical Center, Lexington, KY (S.S.S.).

Correspondence to Susan S. Smyth, MD, PhD, 255 BBSRB, 741 S Limestone St, Gill Heart Institute, Lexington, KY 40536. E-mail susansmyth@uky.edu

Arterioscler Thromb Vasc Biol **is available at http://atvb.ahajournals.org** **DOI: 10.1161/ATVBAHA.111.234708**

quently, nitric oxide levels, as well as endothelin levels, both important regulators of pulmonary vascular tone.[21–23] Thus, LPA has actions on both vascular SMCs and endothelial cells that trigger a dysregulation in their function that is similar to what is observed in a variety of pathological conditions, including PH. However, until recently, tools to probe the role of the autotaxin-LPA signaling nexus in vascular pathophysiology were not available.

Recent progress in identifying enzymes and receptors responsible for LPA metabolism and signaling has enabled the development of mouse models and pharmacological tools to investigate the involvement of LPA in cardiovascular regulation and function. LPA signaling responses are mediated by selective G protein–coupled receptors. Eight G protein–coupled receptors for LPA (LPA_{1-8}) have been identified.[18,20,21,22] LPA_1 and LPA_2 are abundantly expressed in vascular SMCs and endothelial cells.[23,24] In vitro studies in cell lines reveal that LPA receptors share certain function redundancy.[18,19,25] Although a complete range of subtype specific receptor antagonists is not presently available, the use of LPA receptor–selective probes and studies of mice with genetic deletion of LPA receptors have provided valuable information on their pathophysiologic roles in diverse settings, including neuropathic pain, lung inflammation, reproduction, and vascular injury responses.[26] LPA is produced in the blood and other tissues through hydrolysis of lysophosphatidylcholine, catalyzed by the secreted enzyme autotaxin/lysophospholipase D encoded by the ectonucleotide pyrophosphatase/phosphodiesterase 2 (*ENPP2*) gene.[10] *Enpp2*$^{-/-}$ mice die embryonically and display defects on vessel maturation. *Enpp2*$^{+/-}$ mice are viable but have approximately half the normal circulating autotaxin/lysophospholipase D and LPA levels.[27]

Substantial evidence identifies a role for LPA in regulating phenotypic modulation of cultured vascular SMCs that can be recapitulated in vivo by local administration of LPA to systemic arteries.[12,17] The use of mice with genetic deficiencies and small molecule inhibitors of LPA receptors supports a role for the autotaxin-LPA signaling nexus in systemic arterial remodeling in rodent models. In this study, we used mice with alterations in LPA signaling and metabolism and previously characterized models of PH[28] to identify an unexpected role for LPA in regulation of the pulmonary vasculature and hypoxia-induced remodeling.

Methods

All procedures conformed to the recommendations of the *Guide for the Care and Use of Laboratory Animals* (Department of Health, Education, and Welfare publication number NIH 78–23, 1996, University of Kentucky) and were approved by the institutional animal care and use committee. Generation and characterization of *Enpp2*$^{+/-}$ and *Lpar1*$^{-/-}$2$^{-/-}$ mice were as previously described.[27,29–31] The *Enpp2*$^{+/-}$ mice were backcrossed >10 generations to the FVB background, whereas the *Lpar1*$^{-/-}$, *Lpar2*$^{-/-}$, and *Lpar1*$^{-/-}$2$^{-/-}$ mice were backcrossed >10 generations to the BALB/c background. Mice were housed in cages with HEPA-filtered air in rooms on 14-hour light cycles and fed Purina 5058 rodent chow ad libitum. Details of the methods are included in the supplemental materials, available online at http://atvb.ahajournals.org.

Statistics

All results were expressed as mean±SD. In vitro studies were repeated a minimum of 3 times, and results were analyzed by the Student *t* test or ANOVA. Statistical significance within strains was determined using ANOVA with multiple pair-wise comparisons. Statistical analysis was performed using Sigma-STAT software, version 3.5 (Systat Software Inc). Changes with a probability value of less than 0.05 for a type I error were considered significant.[32]

Results

Reduction in Autotaxin/Lysophospholipase D Levels Promotes Hypoxia-Induced Pulmonary Remodeling in Mice

LPA promotes phenotypic modulation of cultured vascular SMCs and systemic arterial remodeling in experimental models.[12,17] To determine whether LPA contributes to remodeling of the pulmonary vasculature, we examined responses in mice engineered to have reduction in LPA synthesis. Heterozygous *Enpp2*$^{+/-}$ mice have 50% of normal plasma LPA levels but no obvious vascular developmental abnormalities.[27] We previously reported lower autotaxin protein levels in the lungs of *Enpp2*$^{+/-}$ mice.[29] In keeping with those observations, *Enpp2* mRNA expression in lungs of *Enpp2*$^{+/-}$ mice was 20±10% that in lungs from wild-type (WT) littermate controls ($P<0.05$). No difference in lung expression of LPA1–5 receptor mRNA was observed in *Enpp2*$^{+/-}$ mice (data not shown).

We used a hypoxia model to stimulate pulmonary vasoconstriction and promote vascular remodeling.[28] Exposure of WT mice to hypoxia ($FiO_2=0.1$) increases pulmonary arterial pressure, which can be monitored by measuring right ventricular systolic pressure (RVSP) (Figure 1A). Following exposure to hypoxia for 3 weeks, a significant increase in RVSP occurred in WT mice (30.3±2.3 mm Hg; n=6) compared with RVSP in age-matched normoxic littermates (25.7±2.1 mm Hg; n=6; $P<0.05$). Under normoxic conditions, *Enpp2*$^{+/-}$ mice displayed an RVSP (23.8±1.8 mm Hg; n=5) similar to that of their WT littermates (Figure 1A). However, following a 3-week exposure to hypoxia, *Enpp2*$^{+/-}$ mice developed higher RVSP (36.2±5.2 mm Hg; n=7; $P<0.05$) than WT littermate mice (Figure 1A). Peak flow velocity across the pulmonary valve decreased by 8.0±5.7% following hypoxia in WT mice. The decline in peak flow velocity was approximately twice as great (16.2±8.4%) in *Enpp2*$^{+/-}$ littermates after exposure to hypoxia (Table 1).

To evaluate the role of pulmonary vascular remodeling in the enhanced RVSP and peak flow response of the *Enpp2*$^{+/-}$ mice to hypoxia, we examined muscularization of small pulmonary arterioles. Lung sections stained with α-smooth muscle actin, a marker for SMCs, were scored for non-, partially, and fully muscularized small pulmonary arterioles. The overall pulmonary histology of *Enpp2*$^{+/-}$ mice was not notably different from WT controls; in particular, WT and *Enpp2*$^{+/-}$ littermates maintained in normoxic conditions did not differ in the percentage of muscularized arterioles. Following a 3-week exposure to hypoxia, the percentage of muscularized small arterioles increased by ≈1.75-fold in WT mice. Lungs from *Enpp2*$^{+/-}$ mice exposed to hypoxia had a higher percentage of fully muscularized and a lower percentage of nonmuscularized distal small arterioles than did those

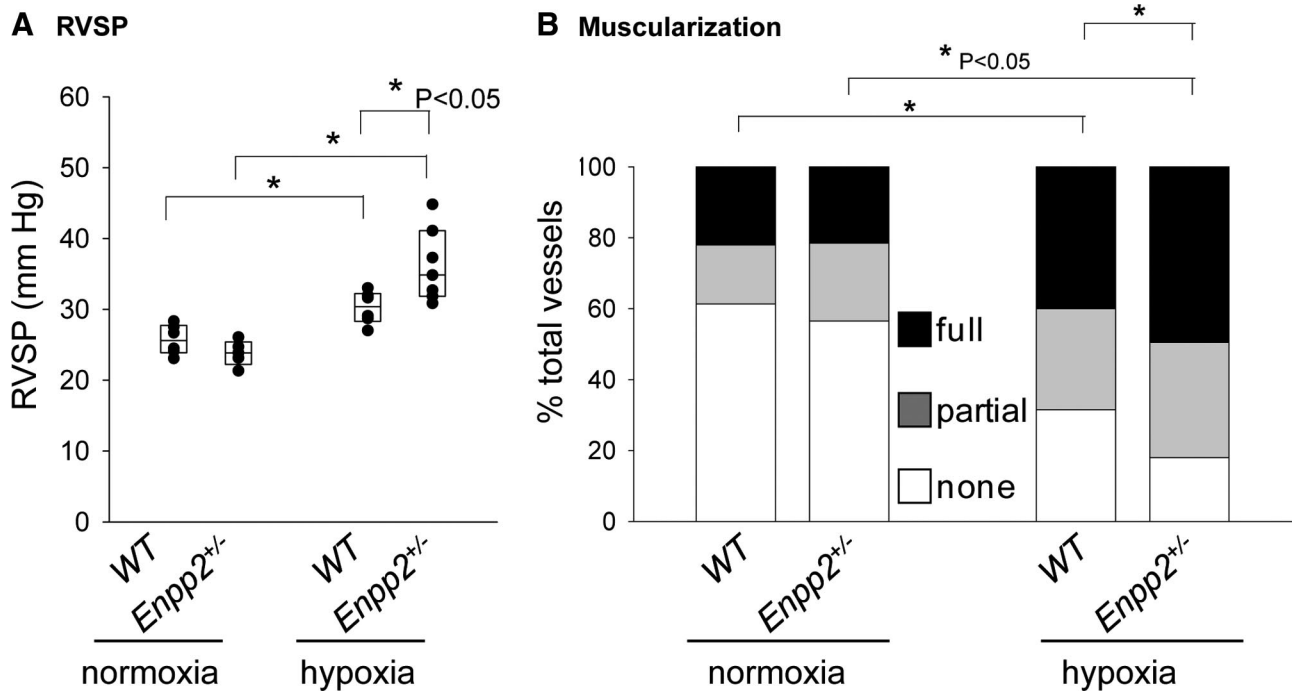

Figure 1. Response of mice with reduced autotaxin levels (*Enpp2*$^{+/-}$) to hypoxia. **A**, Right ventricular systolic pressure (RVSP) of wild-type (WT) (n=6) and *Enpp2*$^{+/-}$ (n=5) mice housed in normoxic conditions and WT (n=6) and *Enpp2*$^{+/-}$ (n=7) mice with 3 weeks of hypoxia exposure. Individual values (dots) and medium with 25 and 75 confidence intervals (box plots) are presented. Data were analyzed by 2-way ANOVA. *$P<0.05$. **B**, Percentage of muscularization of distal pulmonary arterioles in normoxic or hypoxic WT and *Enpp2*$^{+/-}$ mice. Lung sections were immunostained with α-smooth muscle actin and scored as described in Materials and Methods. None indicates nonmuscularized vessels; partial, partially muscularized vessels; full, fully muscularized vessels. Data are presented as averages of 4 mice/group and were analyzed by 2-way ANOVA. The percentages of nonmuscularized vessels were used for statistical analysis. *$P<0.05$.

of WT controls (Figure 1B). Thus, by 3 parameters, *Enpp2*$^{+/-}$ mice showed an exaggerated pulmonary vascular response to hypoxia consistent with an augmentation in hypoxia-induced PH.

Genetic Inactivation of LPA_1 and LPA_2 Promotes Hypoxia-Induced Pulmonary Remodeling in Mice

The exaggerated response of the pulmonary vasculature of *Enpp2*$^{+/-}$ mice to hypoxia suggests that LPA signaling may be protective in this setting. We therefore predicted that inactivation of the relevant LPA receptors would also result in exaggerated remodeling responses to hypoxia. LPA_1 and LPA_2 receptors are reported to be abundantly expressed in cultured endothelial and vascular SMCs.[23,24] We observed relatively high expression in murine blood vessels, making these receptors candidates for mediating the pulmonary vascular remodeling responses. WT and *Lpar1*$^{-/-}$2$^{-/-}$ mice (8–14 weeks old) were subjected to hypoxia for 3 weeks.

Table 1. Peak Flow Velocity Across the Pulmonary Valve Before and After 3 wk of Exposure to Normoxia or Hypoxia

Genotype	Condition	n	Baseline	After 3 wk
Enpp2$^{+/+}$	Normoxia	4	879±44	993±70
Enpp2$^{+/+}$	Hypoxia	6	899±76	824±55
Enpp2$^{+/-}$	Normoxia	5	928±66	923±41
Enpp2$^{+/-}$	Hypoxia	7	961±93	802±95

Results are presented as mean±SD in mm/s.

Exposure of *Enpp2*$^{+/-}$, which are on the FVB background, to hypoxia did not result in mortality. However, the *Lpar1*$^{-/-}$2$^{-/-}$ mice are on the BALB/c background, and ≈10% of the WT mice and ≈55% of the *Lpar1*$^{-/-}$2$^{-/-}$ mice died during the 3-week exposure to hypoxia. The surviving *Lpar1*$^{-/-}$2$^{-/-}$ mice displayed evidence of hemodynamic compromise (heart rate <300 bpm), and therefore, we were unable to obtain accurate RVSP measurements following exposure to hypoxia. Because sustained elevation in RVSP produces RV hypertrophy, we analyzed heart cross-sections to detect RV hypertrophy as an indirect marker for RVSP. In comparison with WT mice, *Lpar1*$^{-/-}$2$^{-/-}$ mice developed more pronounced RV hypertrophy after hypoxia (Figure 2A and 2B). Similar to *Enpp2*$^{+/-}$ mice, the *Lpar1*$^{-/-}$2$^{-/-}$ mice had an approximately 2-fold greater reduction in peak flow velocity across the pulmonary valve after hypoxia than their WT controls (Table 2). Analysis of the lungs revealed significantly more muscularized and fewer nonmuscularized pulmonary arterioles in *Lpar1*$^{-/-}$2$^{-/-}$ mice than in age-matched WT controls (Figure 2C). Likewise, *Lpar1*$^{-/-}$2$^{-/-}$ mice had thicker pulmonary arteriolar walls, suggesting positive arteriolar remodeling (Figure 2D). Together, these results indicate that mice lacking LPA signaling through LPA_1 and LPA_2 receptors were hyperresponsive to hypoxia-induced pulmonary remodeling and RV hypertrophy, providing further support for a protective role of LPA signaling in the pulmonary vasculature and indicating that these effects are mediated by LPA_1 and LPA_2.

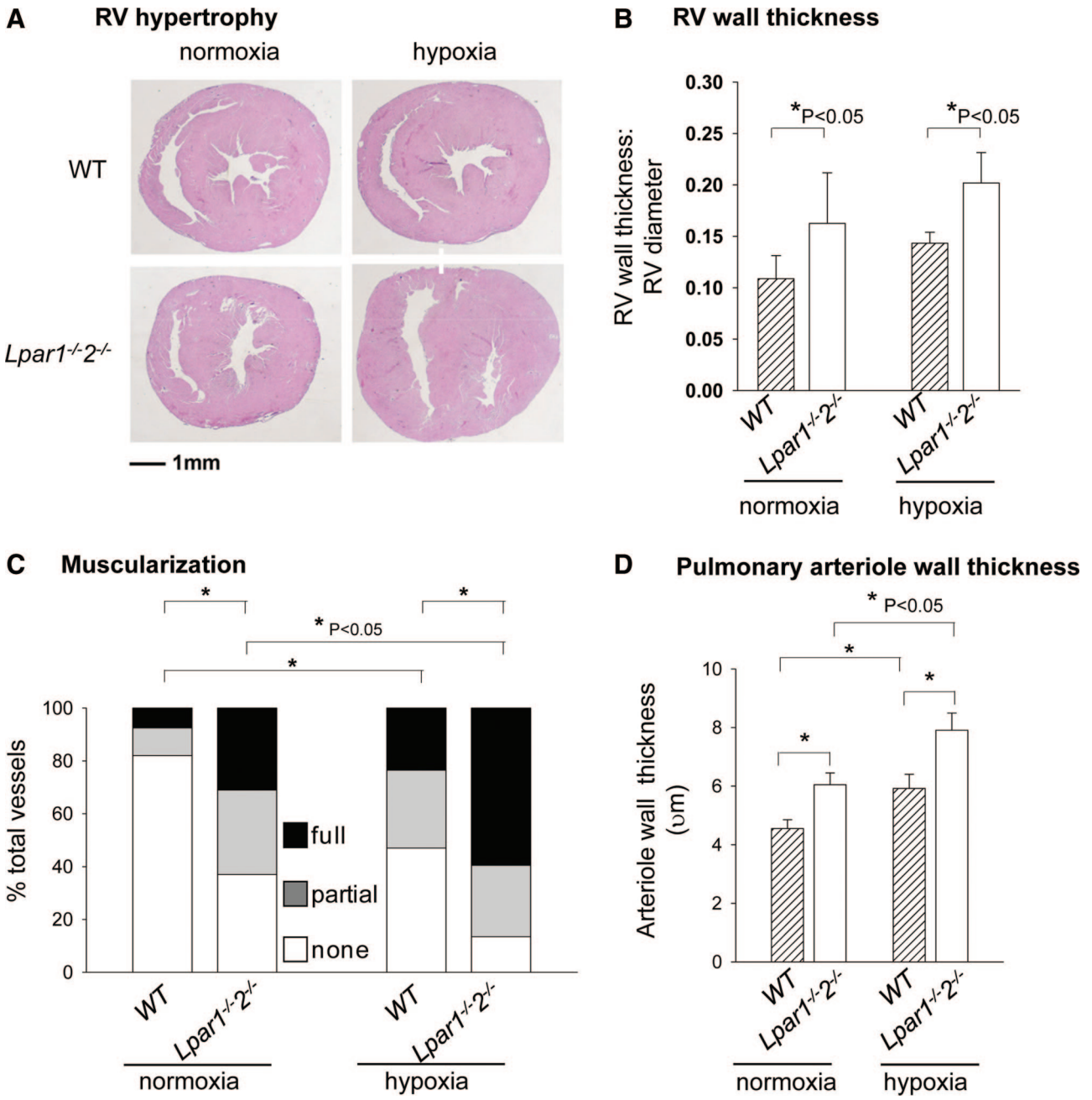

Figure 2. Response of lysophosphatidic acid $(LPA)_1$- and LPA_2- double deficient mice to hypoxia. **A**, Representative cross-section images of hearts from normoxic and hypoxic wild-type (WT) and *Lpar1*$^{-/-}$2$^{-/-}$ mice. Hearts were sectioned at the widest point transversely and stained with hematoxylin/eosin. RV indicates right ventricular. **B**, Quantification of RV free wall thickness to cross-section diameter ratio in normoxic and hypoxic WT and *Lpar1*$^{-/-}$2$^{-/-}$ mice (n=5 per group). **C**, Percentage of muscularization of distal pulmonary arterioles in normoxic and hypoxic WT and *Lpar1*$^{-/-}$2$^{-/-}$ mice. Lung sections were immunostained with α-smooth muscle actin and scored as described in Materials and Methods. None indicates nonmuscularized vessels; partial, partially muscularized vessels; full, fully muscularized vessels. Data are presented as mean±SD from 4 mice/group and were analyzed by 2-way ANOVA. *P<0.05. **D**, Pulmonary arteriolar wall thickness in WT and *Lpar1*$^{-/-}$2$^{-/-}$ mice under normoxic and hypoxic conditions. Data are presented as mean±SD from 4 mice/group. *P<0.05.

Mice Lacking LPA_1 and LPA_2 Develop PH With Age

Under normoxic conditions, the pulmonary arterioles in *Lpar1*$^{-/-}$2$^{-/-}$ mice were more muscularized and thicker than those in WT control mice (Figure 2C and 2D). Changes in elastin content often accompany vascular remodeling. Elastin gene expression (*Eln*) in lungs from *Lpar1*$^{-/-}$2$^{-/-}$ mice was 1.9±0.37-fold higher than in WT controls, and quantification of elastin staining on lung sections confirmed an increase in perivascular elastin content in *Lpar1*$^{-/-}$2$^{-/-}$ mice (Figure 3A–3C). Together, these observations indicate that alterations in the pulmonary vasculature occur in *Lpar1*$^{-/-}$2$^{-/-}$ mice even in the absence of hypoxia. To determine whether these alterations promoted the subsequent development of pulmonary arterial hypertension, we measured RVSP in young and old *Lpar1*$^{-/-}$2$^{-/-}$ mice. Although no significant difference

Table 2. Peak Flow Velocity Across the Pulmonary Valve Before and After 3 wk of Exposure to Hypoxia

Genotype	n	Baseline	After 3 wk
WT	6	633.99±90.22	552±154
Lpar1$^{-/-}$*2*$^{-/-}$	5	607.66±90.78	466±149

Results are presented as mean±SD in mm/s.

in RVSP was observed in WT and *Lpar1*$^{-/-}$2$^{-/-}$ mice at age 8 to 14 weeks (Figure 4A), *Lpar1*$^{-/-}$2$^{-/-}$ mice developed an age-dependent increase in RVSP (58.5±4.5 versus 28.6±8.0 mm Hg in WT mice; $P<0.05$) that did not occur in age-matched *Lpar1*$^{-/-}$ or *Lpar2*$^{-/-}$ mice (Figure 4B). In agreement with the age-dependent elevation in RVSP observed in *Lpar1*$^{-/-}$2$^{-/-}$ mice, peak flow velocity across the pulmonary valve was 11% lower in *Lpar1*$^{-/-}$2$^{-/-}$ (n=18) than in WT (n=22; $P<0.05$) mice at 2 to 3 months of age and declined further in *Lpar1*$^{-/-}$2$^{-/-}$ mice with age, such that by 6 to 9 months of age, the peak flow velocity was 18% lower in the *Lpar1*$^{-/-}$2$^{-/-}$ mice (n=14) than in WT controls (n=11; $P<0.001$) (Table 3). In keeping with the elevated RVSP, histological sections of hearts revealed thicker RV free walls and enlarged RV chambers in older *Lpar1*$^{-/-}$2$^{-/-}$ mice (Figure 4C), which was not observed in *Lpar1*$^{-/-}$ or *Lpar2*$^{-/-}$ mice (Figure 4D). No difference in the number of cardiomyocyte nuclei in the RV was observed in heart cross-sections. The average cross-section area of individual cardiomyocytes in the *Lpar1*$^{-/-}$2$^{-/-}$ RV tended to be larger than in WT mice, but the difference did not reach statistical significance ($P=0.057$) (Supplemental Figure I). We previously reported that systemic blood pressure was normal in *Lpar1*$^{-/-}$2$^{-/-}$ mice.[1] No difference in LV cardiomyocyte size, LV wall thickness, or LV ejection fraction was observed in *Lpar1*$^{-/-}$2$^{-/-}$ mice, suggesting that the alterations were RV specific (Supplemental Figure I and data not shown). No histological evidence of cardiac fibrosis or inflammation was observed in the *Lpar1*$^{-/-}$2$^{-/-}$ cardiac tissue. Taken together, the physiological and histological changes indicate that *Lpar1*$^{-/-}$2$^{-/-}$ mice develop PH and possibly RV hypertrophy spontaneously with age.

We excluded hypoxia as a cause for pulmonary arterial hypertension in *Lpar1*$^{-/-}$2$^{-/-}$ mice. Arterial oxygen saturation in WT mice was 96±1% and 97±1% at 1 to 2 months and 6 months of age, respectively. Corresponding values in the *Lpa1*$^{-/-}$2$^{-/-}$ mice were 95±2%, 97±0.3%, and 96±2% at 1 to 2 months, 3 to 4 months, and >6 months of age, respectively. Additionally, hemoglobin (17.6±1.3 g/dL) and hematocrit (53.3±4.4%) values in *Lpar1*$^{-/-}$2$^{-/-}$ mice did not differ from age-matched WT (17.4±1.6 g/dL and 55.3±7.9%), indicating that the *Lpar1*$^{-/-}$2$^{-/-}$ mice did not develop secondary polycythemia, which would be expected to occur in the setting of prolonged hypoxia (Supplemental Figure II). Because alterations in endothelial permeability have been reported to contribute to the development of PH, we examined pulmonary vascular permeability in *Lpar1*$^{-/-}$2$^{-/-}$ mice. Following intravascular administration, Evans Blue dye accumulation in the lung tissue of WT and *Lpar1*$^{-/-}$2$^{-/-}$ mice was similar after normalization to wet lung weight (Supplemental Figure IIIA). In accordance with Evans Blue data, no histological evidence of edema was seen in the lung tissue of *Lpar1*$^{-/-}$2$^{-/-}$ mice, and wet lung weight/leg bone length was the same in *Lpar1*$^{-/-}$2$^{-/-}$ and WT mice. Examination of pulmonary valves did not reveal any notable abnormalities of *Lpar1*$^{-/-}$2$^{-/-}$ mice, excluding pulmonary stenosis as a cause for the elevated RVSP (Supplemental Figure IIIB). Plastic casting and microcomputed tomography analysis of the pulmonary vasculature also did not reveal obvious obstruction in the structure of the main pulmonary artery (data not shown).

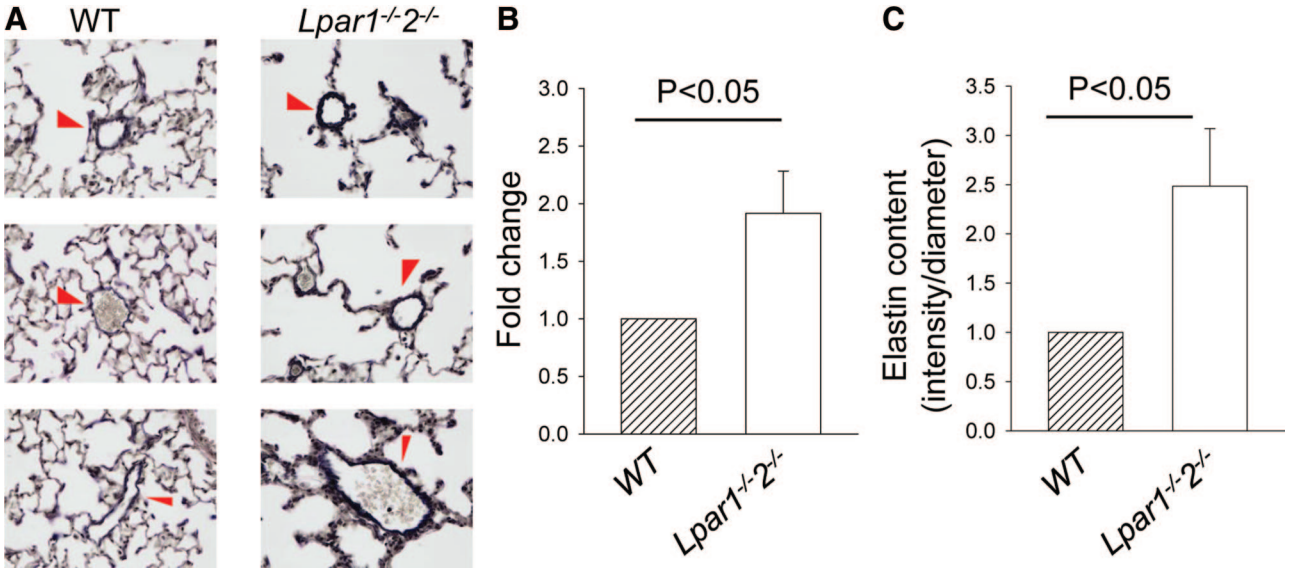

Figure 3. Perivascular elastin deposition in wild-type (WT) and *Lpar1*$^{-/-}$ 2$^{-/-}$ lungs. **A**, Representative images of lung sections of 12-week-old WT and *Lpar1*$^{-/-}$2$^{-/-}$ mice. Sections were stained with elastin staining. Vessels are indicated by arrowheads. **B**, Quantitative reverse transcription–polymerase chain reaction analysis of elastin expression level in lungs of 12-week-old WT (n=3) and *Lpar1*$^{-/-}$2$^{-/-}$ (n=3) mice. The expression level of WT was set as 1, and data are presented as mean±SD. **C**, Quantification of perivascular elastin content in 12-week-old *Lpar1*$^{-/-}$2$^{-/-}$ (n=4) mice and age-matched WT (n=4) mice.

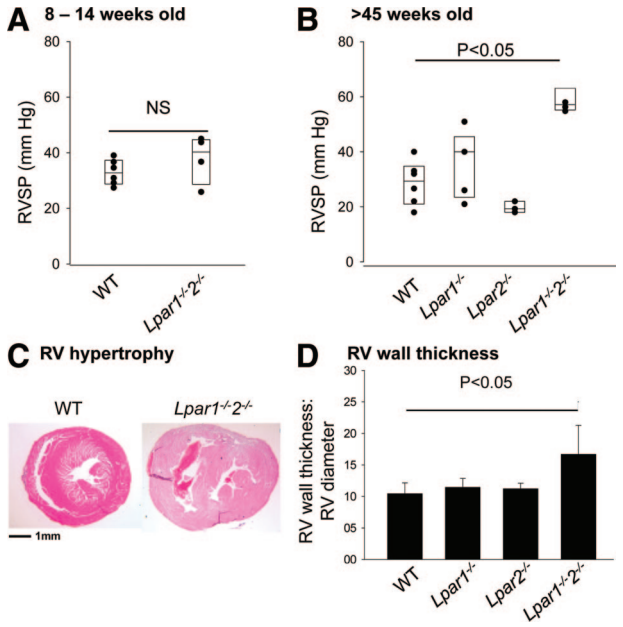

Figure 4. Elevated right ventricular systolic pressures (RVSP) and right ventricular (RV) hypertrophy in older *Lpar1*$^{-/-}$2$^{-/-}$ mice. **A**, RVSP in 8- to 14-week-old wild-type (WT) (n=6) and *Lpar1*$^{-/-}$2$^{-/-}$ (n=4) mice. **B**, RVSP in aged (>45 weeks old) WT (n=6), *Lpar1*$^{-/-}$ (n=5), *Lpar2*$^{-/-}$ (n=3), and *Lpar1*$^{-/-}$2$^{-/-}$ (n=4) mice. Individual values (dots) and medium with 25 and 75 confidence intervals (box plots) are presented. Data were analyzed by 2-way ANOVA. NS indicates not statistically significant. **C**, Representative images of cross-sections of hearts of age-matched WT and *Lpar1*$^{-/-}$2$^{-/-}$ mice (>45 weeks old). Hearts were sectioned at the widest point transversely and stained with hematoxylin/eosin. **D**, Quantification of RV free wall thickness to cross-section diameter ratio of aged (>45 weeks old) WT (n=6), *Lpar1*$^{-/-}$ (n=4), *Lpar2*$^{-/-}$ (n=2), and *Lpar1*$^{-/-}$2$^{-/-}$ (n=6) mice. Data were analyzed by 1-way ANOVA.

In light of the established role of LPA as a stimulus for arterial vascular remodeling and in provoking acute increases in systemic blood pressure in WT and *Lpar1*$^{-/-}$2$^{-/-}$ mice,[1,17] the heightened pulmonary vascular remodeling in mice with attenuated LPA signaling suggested that perhaps LPA has different effects in the systemic and pulmonary vasculature. Therefore, we investigated acute LPA responses in isolated pulmonary-cell and organ models. Analogous to observations in aortic SMCs,[1] LPA stimulated migration of cultured human pulmonary arterial SMCs by 11.6-fold and reduced by 34% expression of SMC-specific myosin heavy chain, a SMC differentiation marker. Infusion of LPA (up to 10 μmol/L) into an isolated buffer-perfused and ventilated mouse lung system did not alter pulmonary artery pressure, under conditions where thrombin (1 U/mL) increased pulmonary artery pressure on average by 130% (from a mean of 5.4±1.2 to 7.1±2 mm Hg). Together, these results suggest that the phenotype observed in the *Enpp2*$^{+/-}$ and *Lpar1*$^{-/-}$2$^{-/-}$ mice may be due to an indirect effect of loss of LPA signaling on another mediator(s).

Table 3. Peak Flow Velocity Across the Pulmonary Valve (PV) of Different Age Groups of *Lpar1*$^{-/-}$*2*$^{-/-}$ Mice

Genotype	Age (mo)	n	PV Velocity
WT	2–3	22	737±76
WT	6–9	11	712±100
Lpar1$^{-/-}$*2*$^{-/-}$	2–3	18	667±152
Lpar1$^{-/-}$*2*$^{-/-}$	6–9	14	584±48

Results are presented as mean±SD in mm/s.

Alterations in Endothelin Signaling in *Enpp2*$^{+/-}$ and *Lpar1*$^{-/-}$2$^{-/-}$ Mice

To understand the basis for the enhanced response in the pulmonary vasculature of mice with attenuated LPA production, we examined expression of mediators implicated in regulating pulmonary vasoconstriction and vasodilation in the *Enpp2*$^{+/-}$ mice. *Vegfr2*, *Pde5a*, and *Nos3* expression were normal in *Enpp2*$^{+/-}$ lungs. Exposure to hypoxia produced a 30% to 40% increase in *Vegfr2* and *Pde5a* expression and a decline of 50% in *Nos3* expression in WT mice. Similar changes occurred in *Enpp2*$^{+/-}$ mice. Exposure to hypoxia increased expression of *Edn1* (encoding for endothelin-1, the most potent vasoconstrictor in the pulmonary circulation) in WT and *Enpp2*$^{+/-}$ by 50%. Hypoxia had no effect on expression of *Ednra* (endothelin [ET]$_A$ receptor) but reduced lung expression of *Ednrb* (ET$_B$ receptor) by 61±11% in WT mice (P<0.05). Interestingly, *Ednrb* expression was 30±1% lower in *Enpp2*$^{+/-}$ than WT mice at baseline (P<0.05) and declined further with hypoxia (P<0.05). On the other hand, the expression levels of *Edn1* and *Ednra* were similar in WT and *Enpp2*$^{+/-}$ mice at baseline or with hypoxia (Supplemental Figure IV). ET$_B$ is a vasodilatory and clearing receptor for endothelin. Reduced levels of ET$_B$ have been associated with acceleration of PH.[33] Thus, an alteration in ET$_B$ expression is a possible explanation for the enhanced remodeling response of *Enpp2*$^{+/-}$ mice. Hypoxia treatment did not have significant effect on the expression levels of *Lpar1* to *Lpar5* in *Enpp2*$^{+/-}$ mice (data not shown).

Next, we examined expression profiles of mediators known to influence development and hypoxia responses in LPA$_1$ and LPA$_2$ deficient mice. In keeping with the observations in *Enpp2*$^{+/-}$ mice, no differences in *Vegfr2*, *Pde5a*, and *Nos3* expression were observed between WT and *Lpar1*$^{-/-}$2$^{-/-}$ mice exposed to normoxic conditions, and both responded with a similar increase in *Vegfr2* and *Pde5a* expression and decline in *Nos3* expression following hypoxia (data not shown). However, the expression levels of *Edn1*, which encodes endothelin-1 (ET-1), and *Ednra,* which encodes the vasoconstrictive ET$_A$ receptor, were significantly higher in *Lpar1*$^{-/-}$2$^{-/-}$ mice than in WT controls (Figure 5A). As in the *Enpp2*$^{+/-}$ mice, *Ednrb* expression was lower in *Lpar1*$^{-/-}$2$^{-/-}$ mice (Figure 5A). The elevation in expression of *Edn1* and *Ednra* and the reduced expression of *Ednrb* were evident as early as postnatal day 3 and persisted at days 7 and 21 and in adulthood. In agreement with mRNA levels, ET-1 peptide content in the lung tissue was also higher in *Lpar1*$^{-/-}$2$^{-/-}$ mice at postnatal day 7 (Figure 5B), and protein levels of ET$_B$ receptor were lower and those of ET$_A$ were higher (Figure 5C and 5D). Given the pronounced vasoconstrictive effects of the endothelin pathway, the changes observed in *Lpar1*$^{-/-}$2$^{-/-}$ mice could account for their propensity to develop pulmonary vascular remodeling and hypertension.

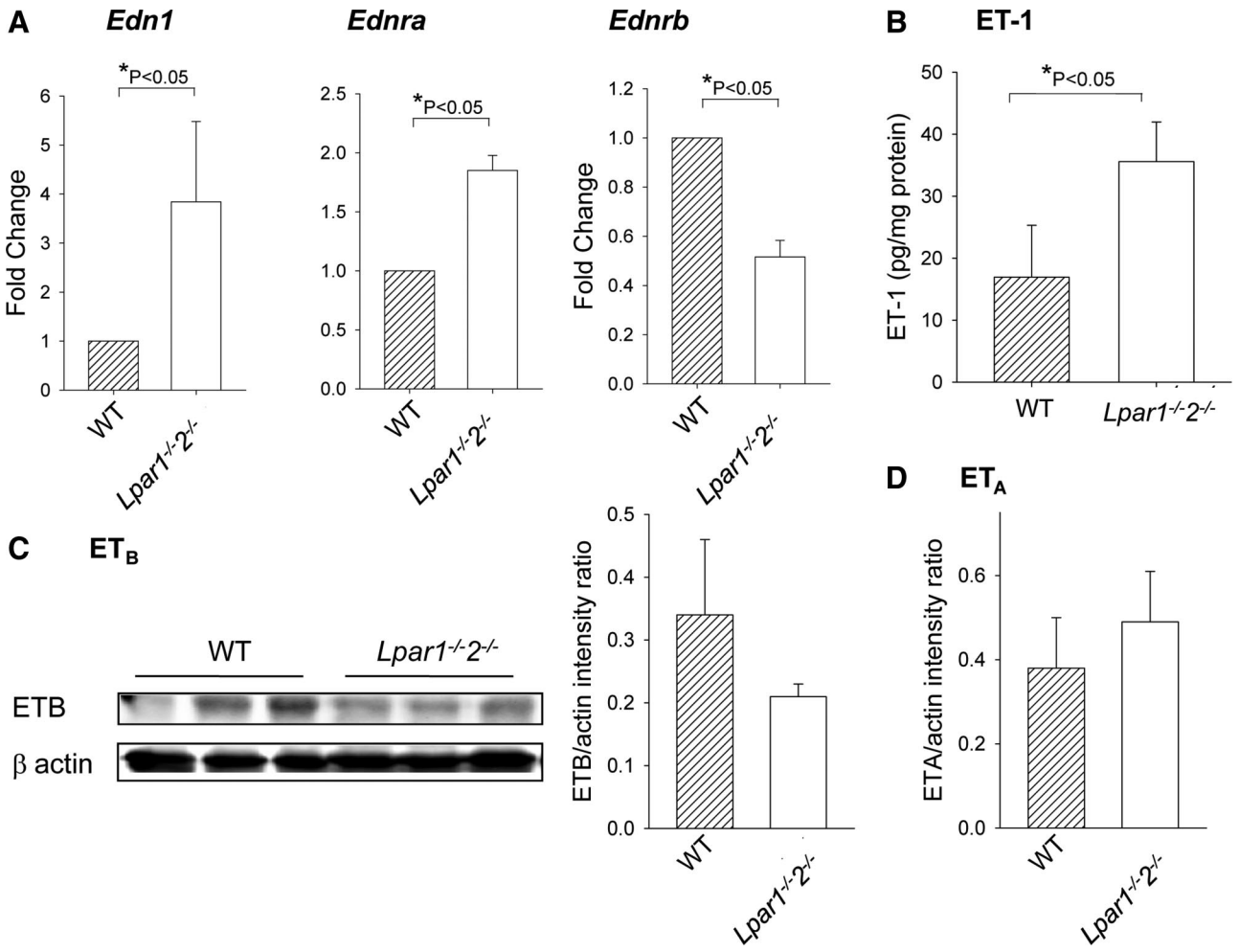

Figure 5. Expression of ET-1 and its receptors in lungs of *Lpar1*$^{-/-}$2$^{-/-}$ mice. **A**, Quantitative reverse transcription–polymerase chain reaction analysis of expression of *Edn1* (encoding ET-1), *Ednra* (ET_A), and *Ednrb* (ET_B) in lungs of age-matched wild-type (WT) (hatched bars) and *Lpar1*$^{-/-}$2$^{-/-}$ (open bars) mice. All results were graphed from 3 experiments and presented as mean±SD. The expression level of WT mice was set as 1. *$P<0.05$. **B**, ET-1 protein content in lungs of age-matched WT (n=5; hatched bars) and *Lpar1*$^{-/-}$2$^{-/-}$ (n=10; open bars) mice. **C** and **D**, ET_B (**C**) and ET_A (**D**) protein levels quantitated by immunoblot analysis and normalized to β-actin expression (n=3 per group). Results are presented as mean±SD.

Discussion

By studying mice with loss-of-function mutations in genes required for LPA production and signaling, we have identified an unanticipated role for this mediator in protection from hypoxia-induced PH. We found that heterozygous inactivation of the LPA-producing enzyme autotaxin promotes the development of hypoxia-induced pulmonary arterial hypertension. Mice lacking LPA_1 and LPA_2 receptors were also more susceptible to hypoxia-induced pulmonary remodeling and spontaneously developed pulmonary arterial hypertension (characterized by elevated RVSP and increased pulmonary arteriolar muscularization and wall thickness) and RV hypertrophy with age. Our findings implicate both LPA_1 and LPA_2 as the main contributors to LPA's effect in the pulmonary vasculature. Because neither *Lpar1*$^{-/-}$ nor *Lpar2*$^{-/-}$ mice display the dramatic development of PH observed in *Lpar1*$^{-/-}$2$^{-/-}$ mice, we conclude that these receptors act redundantly to promote the relevant signaling pathways.

Our findings raise the possibility that LPA has distinct effects in the pulmonary and systemic vasculature. LPA has been widely reported to stimulate cultured SMC migration and proliferation,[13–15] direct LPA administration stimulates neointimal formation in rodent carotid arteries,[17] and systemic LPA administration elevates blood pressure acutely in rodents.[1] Based on its ability to promote migration and dedifferentiation of pulmonary vascular cells, LPA might be predicted to promote or exacerbate PH. LPA_1 and LPA_2 receptors regulate migratory responses in several cell types, including SMCs.[1,34] It is possible that in the setting of attenuated LPA signaling, abnormal SMC migration results in a developmental abnormality of vessel formation that promotes PH. An alternative, but not exclusive, possibility is that LPA signaling plays a fundamental role in maintaining pulmonary vascular tone, and mice with inherited deficiencies in LPA signaling develop compensatory mechanisms to balance the loss of LPA, such as upregulation of endothelin signaling, that contribute to pathology. The ability of LPA to affect acutely systemic blood pressure in certain species was reported more than 30 years ago. However, to our knowledge, this is the first report to document the consequences of long-term deficiency of LPA signaling on vascular tone in an

experimental model. Of interest is the observation that acute LPA administration alters systemic blood pressure but does not affect pulmonary resistance, whereas genetic deficiency in LPA signaling alters the pulmonary vasculature without affecting systemic blood pressure. It is possible that in the absence of LPA signaling, the endothelin pathway is upregulated to maintain systemic pressure at the expense of the pulmonary vasculature. LPA and endothelin share downstream signaling mediators, such as phospholipase C and D, and other work has identified unexpected consequences of genetic deletion of signaling pathways on other systems. Similar effects (for example, those mediated by alterations in coupling of receptors to G protein–coupled receptors) could account for upregulation of endothelin signaling in the absence of LPA receptors.

The development of PH may require several events, including a trigger (such as hypoxia), an imbalance in the ratio of vasodilators to vasoconstrictors, and a permissive genotype.[35] The spontaneous development of PH in the *Lpar1*$^{-/-}$2$^{-/-}$ mice may have been facilitated by permissive genetic modifiers on the BALB/c background. BALB/c mice are more prone than C3H and C57BL/6 mice to developing pulmonary vascular muscularization following smoke exposure.[36] Enhanced hypoxic pulmonary vasoconstriction in BALB/c mice compared with C57BL/6 mice has been observed.[37] The BALB/c background also modifies the phenotype of transforming growth factor-β1-deficient mice,[38] and transforming growth factor-β signaling has been implicated in the development of PH. Differences of baseline cardiovascular phenotypes in mice on various genetic backgrounds are reported and may also explain the differences in peak flow velocity of normoxic *Enpp2* and *Lpar1*$^{-/-}$2$^{-/-}$ mice.[39]

The development of PH in the *Enpp2*$^{+/-}$ and the *Lpar1*$^{-/-}$2$^{-/-}$ mice was likely promoted by an imbalance in the ratio of vasodilators (nitric oxide and prostacyclins) to vasoconstrictors (ET-1 and thromboxane A_2). No difference in expression of enzymes responsible for production of NO (endothelial nitric oxide synthase) or termination of its signaling (phosphodiesterase 5) was observed, nor were there changes in urinary prostacyclin or thromboxane metabolites to account for the development of PH (data not shown). However, in both *Enpp2*$^{+/-}$ and the *Lpar1*$^{-/-}$2$^{-/-}$ mice, lower expression of *Ednrb* could promote pulmonary vasoconstriction. The elevation in ET-1 levels, which occurred in *Lpar1*$^{-/-}$2$^{-/-}$ mice by postnatal day 7, may also contribute to the propensity of these animals to develop PH.

Our findings suggest that there may be significant crosstalk between LPA and endothelin signaling systems that occurs directly or functionally. LPA and ET-1 stimulate many of the same vasoconstrictive and phenotypic changes in cultured SMCs.[40,41] In rat aortic endothelial cells, LPA stimulates pre-proET-1 mRNA levels[42] and, in nonvascular SMCs, some of the effects of ET-1 may be related to production of LPA and signaling through LPA_1.[43] Both LPA and endothelin have been shown to increase blood pressure acutely.[1,44] Thus, in the settings of long-term deficiency of LPA signaling, such as the cases of *Enpp2*$^{+/-}$ and the *Lpar1*$^{-/-}$2$^{-/-}$ mice, compensatory changes in endothelin signaling pathways may occur that promote pathology. Precedent for this exists; mice that are deficient in cyclooxygenase 2 have an upregulation in ET_A receptors and develop exacerbated hypoxia-induced PH.[45] Experiments are under way to elucidate the mechanism(s) of downregulation of *Ednrb* and hence enhanced endothelin signaling in the deficiency of LPA.

In conclusion, by studying mouse models with reduced LPA levels, as well as impaired LPA signaling, we identified important roles for LPA_1 and LPA_2 receptors in pulmonary development and in the maintenance of normal pulmonary vascular pressure. These results focus attention on the possibility that components of the LPA signaling system could be targets for pharmacological treatment of PH.

Acknowledgments

The authors thank Wouter Moolenar of the Netherlands Cancer Institute for his generous gift of *Enpp2*$^{+/-}$ mice.

Sources of Funding

This work was supported by National Institutes of Health Grants HL078663, HL074219 (to S.S.S.), and ARRA supplement (to P.M.), and an American Heart Association predoctoral fellowship (to H.-Y.C.). This work was supported by resources and the use of facilities at the Lexington Veterans Affairs Medical Center.

Disclosures

The authors have no first-tier potential conflicts of interest with the submitted work to report. Dr Smyth has received investigator-initiated research/grant support from AstraZeneca, Boehringer Ingelheim, and the Medicines Company in excess of $50,000 for unrelated work, and her laboratory serves as a core laboratory for pharmacodynamic analysis overseen by CirQuest Laboratories that is part of a preplanned substudy of the TRACER trial.

References

1. Panchatcharam M, Miriyala S, Yang F, Rojas M, End C, Vallant C, Dong A, Lynch K, Chun J, Morris AJ, Smyth SS. Lysophosphatidic acid receptors 1 and 2 play roles in regulation of vascular injury responses but not blood pressure. *Circ Res*. 2008;103:662–670.
2. Humbert M, Sitbon O, Simonneau G. Treatment of pulmonary arterial hypertension. *N Engl J Med*. 2004;351:1425–1436.
3. McLaughlin VV, McGoon MD. Pulmonary arterial hypertension. *Circulation.* 2006;114:1417–1431.
4. De Marco T. Pulmonary arterial hypertension and women. *Cardiol Rev.* 2006;14:312–318.
5. Gaine S. Pulmonary hypertension. *JAMA.* 2000;284:3160–3168.
6. Ferlinz J. Right ventricular diastolic performance: compliance characteristics with focus on pulmonary hypertension, right ventricular hypertrophy, and calcium channel blockade. *Cathet Cardiovasc Diagn*. 1998;43:206–243.
7. Watanabe S. Pathophysiology of hypoxaemic pulmonary vascular diseases. *Bull Eur Physiopathol Respir.* 1987;23(suppl 11):207s–209s.
8. Michelakis ED, Wilkins MR, Rabinovitch M. Emerging concepts and translational priorities in pulmonary arterial hypertension. *Circulation.* 2008;118:1486–1495.
9. Moolenaar WH. Lysophosphatidic acid, a multifunctional phospholipid messenger. *J Biol Chem*. 1995;270:12949–12952.
10. Smyth SS, Cheng HY, Miriyala S, Panchatcharam M, Morris AJ. Roles of lysophosphatidic acid in cardiovascular physiology and disease. *Biochim Biophys Acta*. 2008;1781:563–570.
11. Tokumura A, Fukuzawa K, Tsukatani H. Effects of synthetic and natural lysophosphatidic acids on the arterial blood pressure of different animal species. *Lipids.* 1978;13:572–574.
12. Hayashi K, Takahashi M, Nishida W, Yoshida K, Ohkawa Y, Kitabatake A, Aoki J, Arai H, Sobue K. Phenotypic modulation of vascular smooth muscle cells induced by unsaturated lysophosphatidic acids. *Circ Res*. 2001;89:251–258.
13. Gennero I, Xuereb JM, Simon MF, Girolami JP, Bascands JL, Chap H, Boneu B, Sie P. Effects of lysophosphatidic acid on proliferation and

cytosolic Ca++ of human adult vascular smooth muscle cells in culture. *Thromb Res*. 1999;94:317–326.
14. Boguslawski G, Grogg JR, Welch Z, Ciechanowicz S, Sliva D, Kovala AT, McGlynn P, Brindley DN, Rhoades RA, English D. Migration of vascular smooth muscle cells induced by sphingosine 1-phosphate and related lipids: potential role in the angiogenic response. *Exp Cell Res*. 2002;274:264–274.
15. Damirin A, Tomura H, Komachi M, Liu JP, Mogi C, Tobo M, Wang JQ, Kimura T, Kuwabara A, Yamazaki Y, Ohta H, Im DS, Sato K, Okajima F. Role of lipoprotein-associated lysophospholipids in migratory activity of coronary artery smooth muscle cells. *Am J Physiol Heart Circ Physiol*. 2007;292:H2513–H2522.
16. Yoshida K, Nishida W, Hayashi K, Ohkawa Y, Ogawa A, Aoki J, Arai H, Sobue K. Vascular remodeling induced by naturally occurring unsaturated lysophosphatidic acid in vivo. *Circulation*. 2003;108:1746–1752.
17. Zhang C, Baker DL, Yasuda S, Makarova N, Balazs L, Johnson LR, Marathe GK, McIntyre TM, Xu Y, Prestwich GD, Byun HS, Bittman R, Tigyi G. Lysophosphatidic acid induces neointima formation through PPARγ activation. *J Exp Med*. 2004;199:763–774.
18. Moolenaar WH, van Meeteren LA, Giepmans BN. The ins and outs of lysophosphatidic acid signaling. *Bioessays*. 2004;26:870–881.
19. Ishii I, Fukushima N, Ye X, Chun J. Lysophospholipid receptors: signaling and biology. *Annu Rev Biochem*. 2004;73:321–354.
20. Lee CW, Rivera R, Gardell S, Dubin AE, Chun J. GPR92 as a new G12/13- and Gq-coupled lysophosphatidic acid receptor that increases cAMP, LPA5. *J Biol Chem*. 2006;281:23589–23597.
21. Brinkmann V. Sphingosine 1-phosphate receptors in health and disease: mechanistic insights from gene deletion studies and reverse pharmacology. *Pharmacol Ther*. 2007;115:84–105.
22. Noguchi K, Herr D, Mutoh T, Chun J. Lysophosphatidic acid (LPA) and its receptors. *Curr Opin Pharmacol*. 2009;9:15–23.
23. Lee H, Goetzl EJ, An S. Lysophosphatidic acid and sphingosine 1-phosphate stimulate endothelial cell wound healing. *Am J Physiol Cell Physiol*. 2000;278:C612–C618.
24. Kim J, Keys JR, Eckhart AD. Vascular smooth muscle migration and proliferation in response to lysophosphatidic acid (LPA) is mediated by LPA receptors coupling to Gq. *Cell Signal*. 2006;18:1695–1701.
25. Fukushima N, Ishii I, Contos JJ, Weiner JA, Chun J. Lysophospholipid receptors. *Annu Rev Pharmacol Toxicol*. 2001;41:507–534.
26. Choi JW, Lee CW, Chun J. Biological roles of lysophospholipid receptors revealed by genetic null mice: an update. *Biochim Biophys Acta*. 2008;1781:531–539.
27. van Meeteren LA, Ruurs P, Stortelers C, Bouwman P, van Rooijen MA, Pradere JP, Pettit TR, Wakelam MJ, Saulnier-Blache JS, Mummery CL, Moolenaar WH, Jonkers J. Autotaxin, a secreted lysophospholipase D, is essential for blood vessel formation during development. *Mol Cell Biol*. 2006;26:5015–5022.
28. Ozaki M, Kawashima S, Yamashita T, Ohashi Y, Rikitake Y, Inoue N, Hirata KI, Hayashi Y, Itoh H, Yokoyama M. Reduced hypoxic pulmonary vascular remodeling by nitric oxide from the endothelium. *Hypertension*. 2001;37:322–327.
29. Pamuklar Z, Federico L, Liu S, Umezu-Goto M, Dong A, Panchatcharam M, Fulerson Z, Berdyshev E, Natarajan V, Fang X, van Meeteren LA, Moolenaar WH, Mills GB, Morris AJ, Smyth SS. Autotaxin/lysophospholipase D and lysophosphatidic acid regulate murine hemostasis and thrombosis. *J Biol Chem*. 2009;284:7385–7394.
30. Contos JJ, Fukushima N, Weiner JA, Kaushal D, Chun J. Requirement for the lpA1 lysophosphatidic acid receptor gene in normal suckling behavior. *Proc Natl Acad Sci U S A*. Nov 21. 2000;97:13384–13389.
31. Contos JJ, Ishii I, Fukushima N, Kingsbury MA, Ye X, Kawamura S, Brown JH, Chun J. Characterization of lpa(2) (Edg4) and lpa(1)/lpa(2) (Edg2/Edg4) lysophosphatidic acid receptor knockout mice: signaling deficits without obvious phenotypic abnormality attributable to lpa(2). *Mol Cell Biol*. 2002;22:6921–6929.
32. Barrick CJ, Rojas M, Schoonhoven R, Smyth SS, Threadgill DW. Cardiac response to pressure overload in 129S1/SvImJ and C57BL/6J mice: temporal- and background-dependent development of concentric left ventricular hypertrophy. *Am J Physiol Heart Circ Physiol*. May 2007;292:H2119–H2130.
33. Nishida M, Okada Y, Akiyoshi K, Eshiro K, Takoaka M, Gariepy CE, Yanagisawa M, Matsumura Y. Role of endothelin ETB receptor in the pathogenesis of monocrotaline-induced pulmonary hypertension in rats. *Eur J Pharmacol*. 2004;496:159–165.
34. Komachi M, Damirin A, Malchinkhuu E, Mogi C, Tobo M, Ohta H, Sato K, Tomura H, Okajima F. Signaling pathways involved in DNA synthesis and migration in response to lysophosphatidic acid and low-density lipoprotein in coronary artery smooth muscle cells. *Vascul Pharmacol*. 2009;50:178–184.
35. Archer S, Rich S. Primary pulmonary hypertension: a vascular biology and translational research "work in progress." *Circulation*. 2000;102:2781–2791.
36. Nadziejko C, Fang K, Bravo A, Gordon T. Susceptibility to pulmonary hypertension in inbred strains of mice exposed to cigarette smoke. *J Appl Physiol*. 2007;102:1780–1785.
37. Weissmann N, Akkayagil E, Quanz K, et al. Basic features of hypoxic pulmonary vasoconstriction in mice. *Respir Physiol Neurobiol*. 2004;139:191–202.
38. Gorham JD, Lin JT, Sung JL, Rudner LA, French MA. Genetic regulation of autoimmune disease: BALB/c background TGF-β1-deficient mice develop necroinflammatory IFN-γ-dependent hepatitis. *J Immunol*. 2001;166:6413–6422.
39. Deschepper CF, Olson JL, Otis M, Gallo-Payet N. Characterization of blood pressure and morphological traits in cardiovascular-related organs in 13 different inbred mouse strains. *J Appl Physiol*. 2004;97:369–376.
40. Ediger TL, Toews ML. Synergistic stimulation of airway smooth muscle cell mitogenesis. *J Pharmacol Exp Ther*. 2000;294:1076–1082.
41. Lesh RE, Emala CW, Lee HT, Zhu D, Panettieri RA, Hirshman CA. Inhibition of geranylgeranylation blocks agonist-induced actin reorganization in human airway smooth muscle cells. *Am J Physiol Lung Cell Mol Physiol*. 2001;281:L824–L831.
42. Chua CC, Hamdy RC, Chua BH. Upregulation of endothelin-1 production by lysophosphatidic acid in rat aortic endothelial cells. *Biochim Biophys Acta*. 1998;1405:29–34.
43. Billon-Denis E, Tanfin Z, Robin P. Role of lysophosphatidic acid in the regulation of uterine leiomyoma cell proliferation by phospholipase D and autotaxin. *J Lipid Res*. 2008;49:295–307.
44. Gardiner SM, March JE, Kemp PA, Bennett T. Cardiovascular effects of endothelin-1 and endothelin antagonists in conscious, hypertensive ((mRen-2)27) rats. *Br J Pharmacol*. 2000;131:1732–1738.
45. Fredenburgh LE, Liang OD, Macias AA, et al. Absence of cyclooxygenase-2 exacerbates hypoxia-induced pulmonary hypertension and enhances contractility of vascular smooth muscle cells. *Circulation*. 2008;117:2114–2122.

Supplemental Material

Methods

Hypoxia model

Mice were exposed to oxygen-poor air (hypoxia) at normal atmospheric pressure by placement of their cages in a commercially available chamber (A-chamber, BioSpherix). The mice resided in the chamber for 24 hrs per day for 3 weeks to induce pulmonary hypertension and vascular remodeling, and were removed from the chamber only for cage, food, and water changes. The hypoxic environment within the chamber was achieved by inflow of compressed nitrogen gas. The oxygen concentration (FIO_2 = 0.10) was controlled by a commercially available oxygen controller (Proox model 110, BioSpherix). Prior and after 3 weeks of hypoxia treatment, echocardiography was performed to evaluate the cardiac function. RV pressures measurements were performed in both normoxic and hypoxic groups. Mice were then euthanized, and organs were collected for histological, biochemical, and gene expression analysis.

Echocardiography

Transthoracic echocardiography was performed using a 30 MHz probe and the Vevo 770 Ultrasonograph (VisualSonics). Mice were lightly anesthetized with 0.8% isoflurane, maintaining heart rate at 400–500 beats/min. The hair was removed from the chest using a chemical hair remover (Nair®). The heart rate and body temperature were maintained and recorded. Two-dimensional parasternal long- and short-axis views were obtained. For determining the flow across the pulmonary valve, high short-axis view was obtained at the level of the right ventricular outflow tract (RVOT) and in which the pulmonary valve can be easily seen. The Doppler mode cursor was positioned at the end of the pulmonary valve to record the peak velocity across the pulmonary valve.

RV pressure measurement

Under anesthesia (inhaled isoflurane 1 – 3%), the mouse was fixed in a supine position with tape on a mouse pad that has imbedded EKG electrodes and surface mounted semi-conductor temperature sensor that distributes heat through surface mounted resistors. Rectal temperature was monitored. Under direct visualization of the trachea, an endotracheal tube was inserted and connected to a Harvard rodent volume-cycled ventilator (Model 645, Harvard Apparatus) via the Y-shaped connector. Ventilation was performed with a tidal volume of 200 μL and a respiratory rate of

150/min. Oxygen was provided to the inflow of the ventilator. The chest cavity was opened by an incision of the left fourth intercostal space. An 1 French catheter (Millar Instruments) was quickly inserted into the RV and pressure traces was obtained by Chart 5 Pro (AD Instruments). The animal was euthanized while still under anesthesia, and organs were obtained for histology and RT-PCR analysis.

Real-time PCR

Lungs were collected from mice and weighed. A representative piece from taken from similar locations in each lung was immediately cut and stored in RNAlater (Qiagen). The tissues were homogenized by mortar and pestle, and total RNA was extracted using Trizol (Invitrogen) following manufacturer's instructions. cDNA was prepared with Multiscribe reverse-trasncriptase enzyme as per manufacturer's directions (High-Capacity cDNA Archive Kit; Applied Biosystems). mRNA expression was measured in real-time quantitative PCR using the following predesigned TaqMan® gene expression assays (Applied Biosystems): mouse genes- *Enpp2* (Mm00516572_m1), *Eln* (Mm00514670_m1), *Edn1* (Mm00438656_m1), *Ednra* (Mm01243722_m1), *Ednrb* (Mm00432989_m1), *Vegfr2* (Mm01222419_m1), *Pde5a* (Mm01324391_m1), *Nos3* (Mm00435204_m1), *Lpar1* (Mm00439145_m1), *Lpar2* (Mm00469562_m1), *Lpar3* (Mm00469694_m1), *Lpar4* (Mm01228532_m1), *Lpar5* (Mm01190818_m1). All the probes used in the study spanned an exon junction and thus would not detect genomic DNA. An RNA sample without reverse transcription was used as a negative control. Samples were assayed on an ABI Prism® 7500 Fast Real-Time PCR System. Threshold cycles (C_T) were determined by an in-program algorithm assigning a fluorescence baseline based on readings prior to exponential amplification. Fold change in expression was calculated using the $2^{-\delta\delta CT}$ method using 18s RNA as an endogenous control.

Histology

Mice were weighed, and hearts, lungs, livers, and kidneys were dissected, rinsed in PBS, and weighed. Hearts were cut in a cross section at the widest point. The top half of the heart was fixed with 4% paraformaldehyde and embedded in paraffin. 5 μm sections of hearts and lungs were prepared with microtome. The sections were stained with hematoxylin and eosin for examination of gross appearance, whereas Masson's Trichrome, periodic acid-Schiff, and van Gieson counterstained with hematoxylin (PAS-H) was employed to facilitate quantification of fibrosis, cardiomyocyte size, and elastin content respectively. Cardiomyocyte hypertrophy was assessed by measuring cross-sectional area of 50 cardiomyocytes per PAS-H-stained section in randomly selected fields having nearly circular capillary

profiles and centered nuclei in the LV or RV free walls. The morphology, muscularization percentage of small arterioles, and arteriolar wall thickness were quantified with lung sections immunostained with the biotinylated anti-α-smooth muscle actin antibody (Sigma Chemical Co.). Small arterioles with diameters ranging in 15-100 μm are scored. Arterioles with no positive α -smooth muscle actin staining are characterized as non-muscularized, wrapped with 0-75% positive staining as partially-muscularized, and >75% positive staining as fully-muscularized vessels. 50 arterioles in each section were counted. The percentages of non-muscularized vessels were used for statistical analysis. Arteriolar wall thickness and elastin content were quantified with Metamorph imaging software.

Hematological analysis

Retro-orbital bleeding was performed with mice anesthetized with isoflurane. Whole blood was collected into EDTA-coated tubes. Hemoglobin concentration and hematocrit were analyzed with ABC vet hematology analyzer (ABX) set to measure mouse blood cell parameters.

Pulmonary vascular permeability

Mice were kept anesthetized with pentobarbital. The neck skin was cut open, and 1% Evans blue in PBS was injected into the right jugular vein (100 μl / mice). 15 minutes later, heparin with PBS was perfused from RV to LV at a constant rate of 111.8 ml/hr (25 mmHg pressure). The perfused lung was dissected, weighed and immersed in 1ml formamide to extract Evans blue. The extraction was performed in a shaking water bath at 56°C for 24 hours. The extracted Evans blue was quantified by reading absorbance at 600 nm and normalized to lung weight.

Quantification of Endothelin-1, ET_A and ET_B protein

Lung tissues from postnatal day 7 old mice were homogenized with buffer containing 1% NP-40 and centrifuged at 13,000 rpm for 5 minutes to collect supernatant. The homogenized lungs were analyzed as a single batch for ET-1 by ELISA (R&D Systems, Minneapolis, MN) as described in the manufacturer's protocol. Immunoblot analysis was performed with antibodies to ET_A and ET_B (Abcam) and the processed for quantification using the Odyssey infrared imaging system (LI-COR, Lincoln, NE, USA). The results are presented as the intensity of ET receptor to that of β-actin.

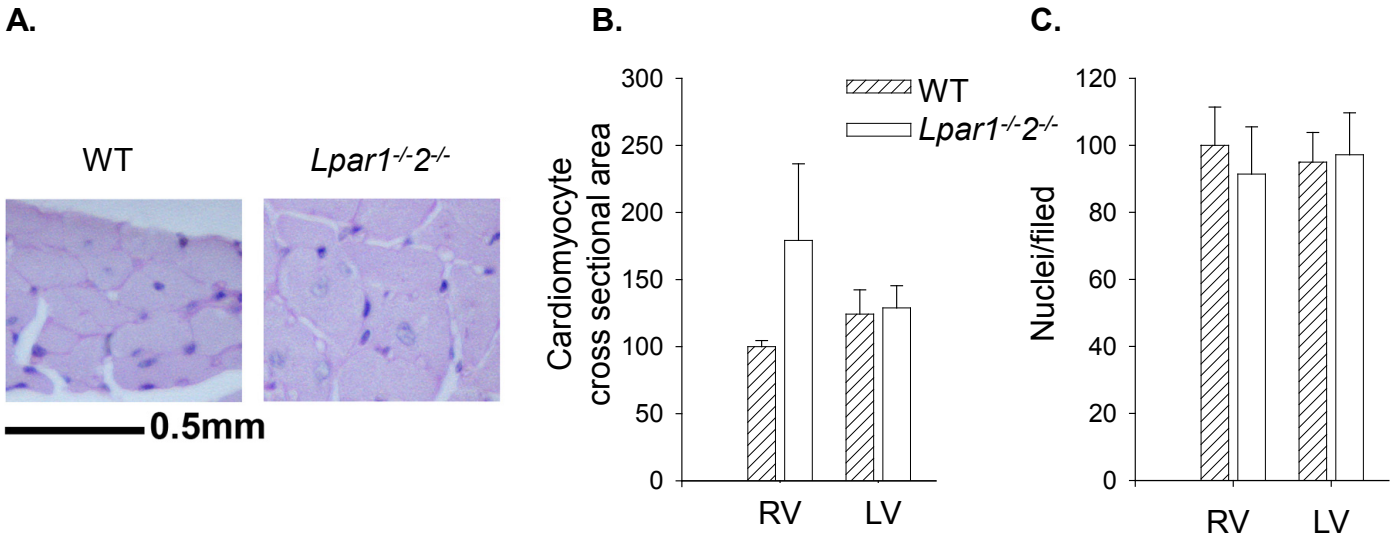

Supplementary Figure I. Cardiomyocyte hypertrophy in older *Lpar1*$^{-/-}$*2*$^{-/-}$ mice.
A. Representative images of RV cardiomyocytes in >45 week old age-matched WT and *Lpar1*$^{-/-}$*2*$^{-/-}$ mice. Hearts were sectioned at the widest point transversely, and stained with PAS. B. Cross-sectional area of individual cardiomyocytes in RV and LV of age-matched (>45 weeks old) WT (n=3) and *Lpar1*$^{-/-}$*2*$^{-/-}$ (n=4) mice. C Average number of cardiomyocytes/field in RV and LV of the same sets of WT (n=3) and *Lpar1*$^{-/-}$*2*$^{-/-}$ (n=4) mice.

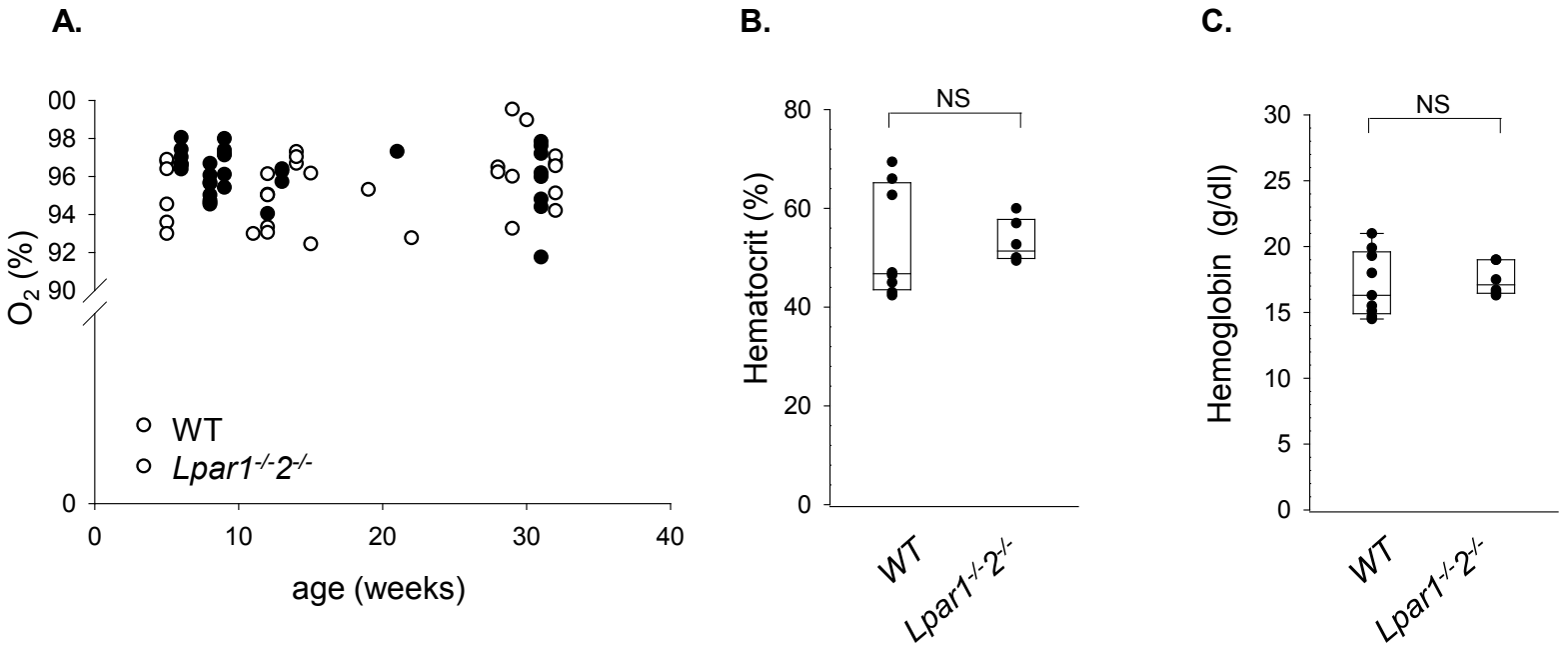

Supplementary Figure II. Normal arterial oxygen saturation, hematocrit , hemoglobin in *Lpar1*$^{-/-}$*2*$^{-/-}$ mice. A. Arterial oxygen saturation percentage (O_2 %) in WT (closed circle) and *Lpar1*$^{-/-}$*2*$^{-/-}$ (open circle) mice at 8 to 32 weeks old. B. Hematocrit (HCT %) of > 27 week-old age-matched WT (n=8) and *Lpar1*$^{-/-}$*2*$^{-/-}$ (n=6) mice. Data are presented as individual values and box plot with median with 25 to 75% confidence intervals. Data were analyzed by t-test. C, Hemaglobin concentration of > 27 week-old age-matched WT (n=9) and *Lpar1*$^{-/-}$*2*$^{-/-}$ (n=6) mice. Data are presented as individual values and box plot with median with 25 to 75% confidence intervals. Data were analyzed by t-test. NS: not statistically significant.

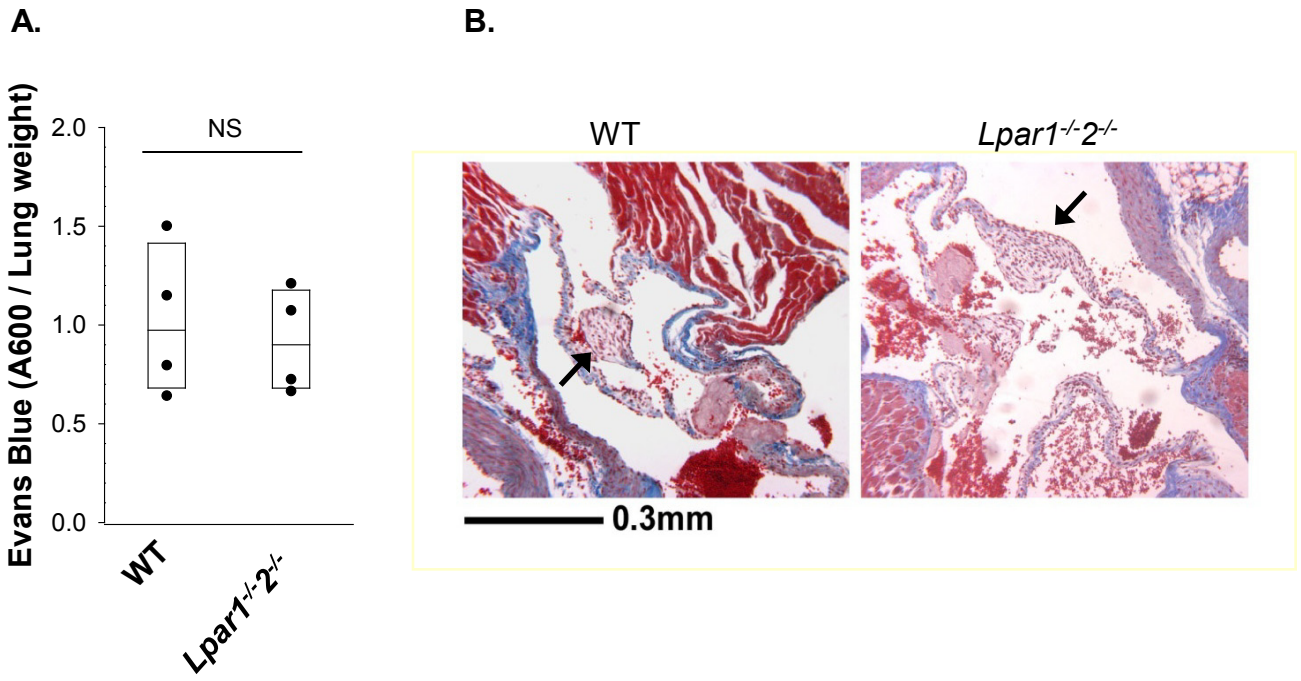

Supplementary Figure III. Normal lung permeability and pulmonary valve architecture in *Lpar1*$^{-/-}$*2*$^{-/-}$ mice. A. Evans blue extracted from lung of age-matched (~24 weeks old) WT (n=4) and *Lpar1*$^{-/-}$*2*$^{-/-}$ (n=4) mice. Individual values (dots) and medium with 25 and 75% confidence intervals (box plots) are presented. Data were analyzed by t-test. NS: not statistically significant. B. Representative images of heart sections at the level of pulmonary valves in WT and *Lpar1*$^{-/-}$*2*$^{-/-}$ mice. Sections were stained with Masson's trichrome staining. Pulmonary valves are indicated by arrows.

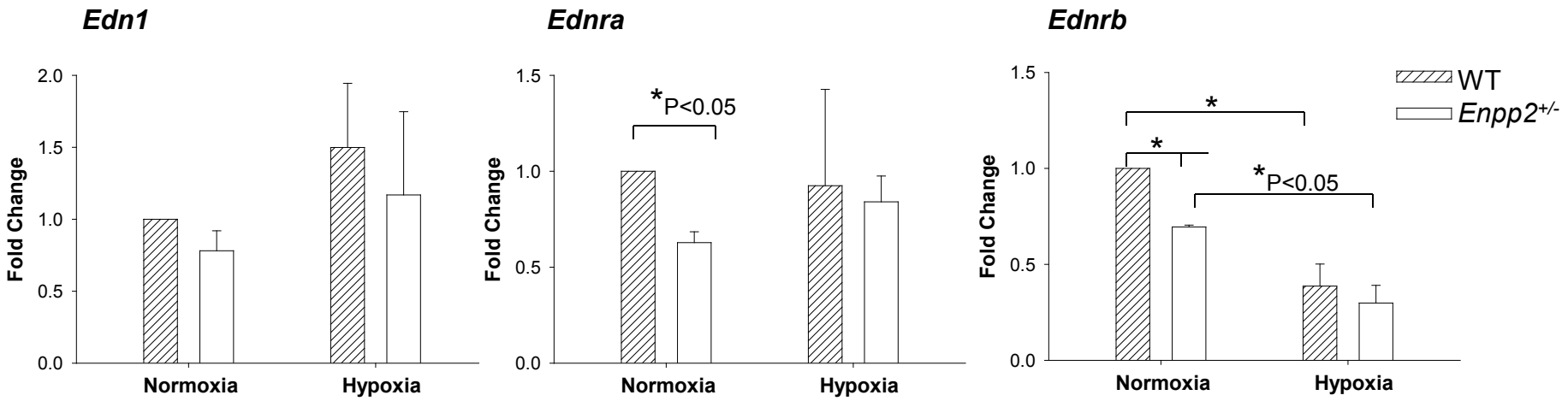

Supplementary Figure IV. Expression of ET-1 and its receptors in lungs of *Enpp2*$^{+/-}$ mice.
Quantitative RT-PCR analysis of expression of *Edn1*(encoding ET-1), *Ednra* (ET_A) and *Ednrb* (ET_B) in lungs of age-matched WT (slashed bars) and *Enpp2*$^{+/-}$ (open bars). Mice under normoxic and hypoxic conditions. All results were graphed from four experiments and presented as mean ± S.D. The expression level of WT mice at normoxia is set as 1. *P<0.05.